ICES Journal of Marine Science, 60: 147–154. 2003
doi:10.1006/jmsc.2002.1327,

A comparison of lidar and echosounder measurements of fish schools in the Gulf of Mexico

James H. Churnside, David A. Demer, and Behzad Mahmoudi

Churnside, J. H., Demer, D. A., and Mahmoudi, B. 2003. A comparison of lidar and echosounder measurements of fish schools in the Gulf of Mexico. – ICES Journal of Marine Science, 60: 147–154.

In December 2000 the US National Oceanic and Atmospheric Administration's Fish Lidar (Light Detection And Ranging) system was operated from an airplane off the west coast of Florida. Schools of fish were located and their volume-backscattering coefficients, $\beta(\pi)$, measured at the lidar wavelength of 532 nm. Concurrently, a 208 kHz echosounder was deployed from a small boat to measure the acoustic volume-backscattering coefficients, s_v, of the same schools. Seven schools were characterized with both the lidar and the echosounder. The correlation between these seven pairs of $\beta(\pi)$ and s_v measurements was 0.994. A linear regression of $\beta(\pi)$ versus s_v had a negative y-intercept, which supports aerial observations of some degree of avoidance reaction of fish to the passing survey boat. The slope was slightly greater than unity, in agreement with previous calculations that the acoustic backscatter of similar fish is slightly greater than the lidar backscatter. The results of this study indicate that lidar is a suitable tool for surveying rapidly the distributions and abundances of epipelagic fish stocks in the shallow waters off the west coast of Florida. Aerial lidar surveys do not have the biases of fish-avoidance reaction potentially affecting acoustic and trawl surveys.

Published by Elsevier Science Ltd on behalf of International Council for the Exploration of the Sea.

Keywords: echosounder, fish, lidar, survey, volume backscatter coefficient.

Received 7 March 2002; accepted 13 October 2002.

J. H. Churnside: NOAA/Environmental Technology Laboratory, 325 Broadway, Boulder, CO 80305, USA. D. A. Demer: NOAA/NMFS/SWFSC/Fisheries Resources Division, 8604 La Jolla Shores Drive, La Jolla, CA 92037, USA. B. Mahmoudi: Florida Marine Research Institute, 100 8th Ave. SE, St Petersburg, FL 33701, USA.

Introduction

There is a critical need to develop rapid and cost-effective methods for assessing living marine resources off the coast of Florida. Fishery resources such as snappers/groupers, mackerels, jacks, tunas, and drums are the backbone of Florida's multi-billion-dollar commercial and recreational fishing industries and require management. Additionally, small pelagic fish such as sardines and herring are vital components of the food chain in the coastal ecosystem. Traditional methods of stock assessment based on long-term fishery and biological data, are inadequate for rapid assessments of fishery resources. These approaches are especially unsatisfactory when immediate estimates of fish-stock biomasses and distributions are needed in cases of environmental catastrophes (e.g. oil spills, severe red tides) and other situations where emergency actions are required.

Consequently, to manage effectively the coastal fisheries for sustainable yield, it is necessary to determine the geographic extent and seasonal abundance and availability of fish stocks using rapidly deployable, fishery-independent methods. Significant advances in quasi-synoptic, fishery-independent survey methods (e.g. aerial-visual, photogrametric, and infrared photogrametric observations, and ship-based hydroacoustic surveys) have recently been made. The Florida Fish and Wildlife Conservation Commission (FFWCC) conducts acoustic/trawl surveys annually to assess fisheries resources along the west coast of Florida. Although these surveys have proven to be an effective method for monitoring interannual stock-size dynamics they are

1054–3139/03/030147+08 $30.00/0

costly and generally too inefficient for rapid assessment purposes.

In response to this perceived remote sensing requirement, the US National Oceanic and Atmospheric Administration's (NOAA) Environmental Technology Laboratory (ETL) has developed a lidar using pulsed-laser light for airborne surveys of fish schools. This lidar has the potential to combine the advantages of active-acoustic systems and aerial-visual techniques. That is, lidar allows the three-dimensional attributes of subsurface fish schools to be measured in a way that takes advantage of the speed provided by an aircraft.

Squire and Krumboltz (1981) demonstrated that fish schools could be detected with an airborne lidar. Krekova *et al.* (1994) presented the results of numerical modeling showing that useful information about fish schools could be extracted from the lidar returns. Churnside *et al.* (1997) successfully tested a lidar system from a ship and made target-strength measurements on live sardines in a tank to demonstrate that biomass estimates were possible. Churnside *et al.* (2001a) presented the results of several tests operating the lidar from various aircraft.

Due to numerous differences between the transmission, propagation, scattering, and receiving characteristics of the two different pulse-echo techniques (lidar and echosounder), the relative accuracy of the lidar measurements is uncertain. The aim of this study is to compare *in situ* volume-backscattering strengths, measured optically versus acousticly, for several fish schools of varying species. Following common usage, the optical volume-backscattering strength is denoted by $\beta(\pi)$, and the acoustic quantities by s_v for the linear value and S_v for the corresponding value in dB. Note that β and s_v are equivalent quantities.

Methods

NOAA's fish lidar system is non-scanning and radiometric (Churnside *et al.*, 2001a). "Non-scanning" means that the angle of incidence of the beam on the water is fixed as long as the plane is flying straight and level. Radiometric means that the absolute level of the reflected laser light is measured. A block diagram is presented in Figure 1. The major components are first, the laser and beam-control optics, second, the receiver optics and detector; and third, the data-collection and display computer. The receiver telescope and the laser are mounted side-by-side and the system was aimed downward through a camera port in the bottom of the NOAA Twin-Otter aircraft flying at an altitude of 300 m. To reduce direct surface reflections the lidar was directed at an angle of 15° from nadir.

The laser used was a Neodymium-doped Yttrium Aluminium Garnet (Nd:YAG). It has a fast optical switch (known as a Q-switch) that is opened after the laser crystal is fully charged so that all of the energy is extracted in a short pulse. It also has a non-linear optical crystal to convert the laser light from infrared (1064 nm) to green (532 nm). This laser produces about 100 mJ of green light in a 12 ns pulse at a repetition rate of 30 Hz. The laser is polarized linearly and the beam is diverged using a lens in front of the laser. The divergence is chosen so that the irradiance at the sea surface satisfies the United States of America's standard for exposure to laser light in the workplace (ANSI, 1993). This irradiance level is also safe for marine mammals (Zorn *et al.*, 2000). The diverged beam is directed by a pair of mirrors to be parallel to the axis of the telescope.

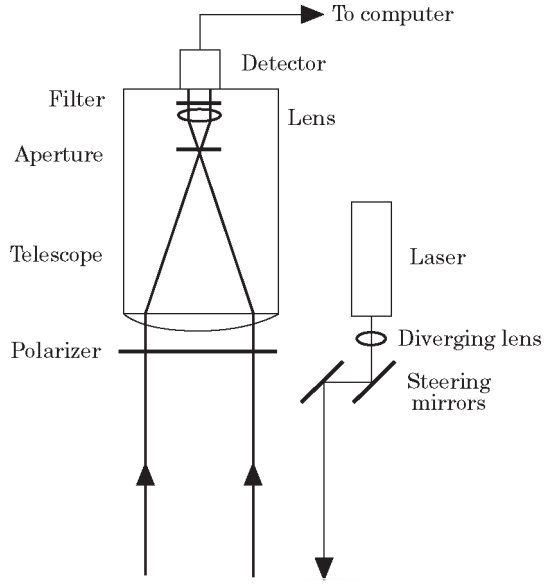

Figure 1. Block diagram of NOAA fish lidar.

The receiver optics comprise a 17 cm diameter refracting telescope with a polarizing filter. The filter passes only that component of the reflected light for which the linear polarization is orthogonal to the polarization of the laser. The cross-polarized component was used because it produces the best contrast between fish and smaller scatterers in the water. This was determined during ship tests of the lidar, where the depolarization of the return from fish was about 30% and the depolarization of the water return was only about 10% (Churnside *et al.*, 1997).

To reject background light the light collected by the telescope passes through an interference filter. Background light is also reduced by an aperture at the focus of the primary lens that matches the field of view of the telescope with the divergence of the transmitted laser beam. The resulting light is incident on a photomultiplier tube (pmt), which converts the light signal into an electrical current. A 50 Ω load resistor converts

the current signal to a voltage which is transformed with a logarithmic amplifier and digitized at 1 GHz with 8 bits of resolution (256 levels). This sample rate corresponds to a resolution of 0.11 m in depth. The amplifier has an input voltage range from -0.2 mV to -2 V that produces an output voltage range of about -0.024 V to -0.524 V, which implies $V_{out} = -0.125 \log(-V_{in}) - 0.486$. Since the output voltage range is well within the range of an 8-bit digitizer the logarithmic amplifier increases the maximum possible dynamic range from 256 to about 10^4.

In addition to the log-transformed voltage signal the computer records the aircraft position from the Global Positioning System (GPS), GPS time, the voltage applied to the pmt and the attitude of the aircraft as measured by tilt sensors and laser gyroscopes on the optical package. The pmt-applied voltage is used to calculate the gain of the tube which is necessary for calibration. The computer also displays the data in real time during the flight. Thus during the pass of the aircraft over a school it is immediately evident whether or not the laser hit the target.

The acoustic system was a Biosonics DT4000 operating a 208 kHz split-beam transducer with a circularly symmetric 6.3° beam width between half-power points. The system was deployed from a 9.5 m skiff and the transducer was mounted on a retractable pole. During the surveys sound pulses of 1 ms duration were transmitted at a rate of approximately 6 Hz. The source level was 221.1 dB with a receiver sensitivity of -52.5 dB. Volume-backscattering strength (S_v) data were indexed with geographic positions and time using a GPS. The water temperature, salinity, and sound absorption at 208 kHz were estimated to be 17.5°C, 35.6 ppt, and 46.6 dB/km, respectively.

Five flights were made out of MacDill Air Force Base, Tampa, Florida, from 4–8 December 2000. During each flight the following sequence was followed: an expert spotter on the aircraft located a school of fish visually, the lidar was repeatedly flown over the targeted school and the boat with the echosounder was directed to the school. Several passes were made over each school with each pass being as close as possible to the centre of each school. Samples were collected then from each school with a hook-and-line (Subiki rig) to get species and size. Although many schools were observed with lidar that were not visible from the aircraft it was impossible to direct the boat to these locations. Therefore, only fish schools that were visible from the air were used in this study.

The first flight covered an area just south of the mouth of Tampa Bay shortly after a storm passed through the area. The coastal waters had a rough surface and were very turbid. Despite these conditions several schools of striped mullet (*Mugil cephalus*) were observed visually moving offshore to spawn. No bait fish were found. Much of the flight was devoted to developing a technique for crossing the schools with the aircraft so that the lidar beam passed through the schools. Toward this end, the lidar beam was adjusted after the first flight to intersect the sea surface slightly forward of the aircraft instead of slightly behind, although the incidence angle was not changed from 15°. During this flight, a protocol was also established for using radio communications and GPS coordinates to direct the boat over the same schools targeted by lidar.

The second flight covered a wider area. Mullet were still in the area but again no bait fish were found. Multiple lidar passes and acoustic measurements were made on one of the mullet schools. A purse seiner circled this school so that echosounder data could be collected on the captive school. Fishing regulations precluded landing the school to get the total biomass measurements.

The third and fourth flights were made to the south of Tampa Bay where bait fish were reported. The species in the samples were Spanish sardine (*Sardinella aurita*), Atlantic thread herring (*Opisthonema oglinum*), blue runner (*Caranx crysos*), and scaled sardine (*Harengula juguana*). Concurrently, the boat with the echosounder was launched near the targeted area. Several schools of fish were located very close to the shore and measured with both the lidar and echosounder. The location was too distant from Tampa Bay for the purse-seine boat to participate. The fifth and final flight was also made to the south of Tampa Bay but farther from shore. Several schools were found in the clearer and deeper water. The water in this area was about 17 m deep with a Secchi depth of 9 m while the region of the previous 2 days had a water depth of about 9 m and a Secchi depth of 4.5 m. Secchi depth is a measure of water clarity given by the depth at which a 30 cm diameter, white disk can no longer be seen from the surface (Shifrin, 1988).

The lidar data were post-processed using the median algorithm described in Churnside *et al.* (2001a). Using this algorithm, the median backscatter intensity in each 0.11 m depth bin for 500 lidar pulses or shots was used to estimate the background level, or the backscattering from essentially empty water. This estimation was valid for the data used in this study as the fish schools occupied far fewer than half the shots at any depth. The background level was subtracted from the return of each lidar shot and the difference was interpreted to be the backscatter from fish schools; at the edges of the school this difference is less than zero.

Calibration was performed at the Department of Commerce's Table Mountain facility north of Boulder, Colorado. The calibration target is a 0.203 m by 0.254 m Kodak gray card (Catalog number E152 7795), which has a reflectance of 18% across the visible. Measurements showed that this target totally depolarized the reflected light, so the reflectance of

cross-polarized light is 9%. The manufacturer claims a maximum deviation in reflectance of 1%. The surface of the card is rough compared with the wavelength of light so the angular dependence of the reflectance of normally incident light has the cosine shape characteristic of a Lambertian reflector. The card was mounted vertically 300 m from the lidar. The energy density of the incident laser was measured just in front of the target. This, divided by the total transmitted energy, indicated that the card intercepted 4.6% of the total energy. Thus, the total reflectivity of our calibration geometry was 0.41%.

To avoid saturation the lidar was calibrated with reduced laser energy, the addition of a known absorber in front of the detector and reduced detector gain. The peak signal was recorded under these conditions. During the experiment the laser power and detector gain were recorded and the peak signals from the fish schools were measured. We define the Lambertian reflectivity of each school as the reflectivity that we calculate as if the school were a diffuse target. This is calculated from:

$$R_L = 0.0041 \frac{0.0393}{E_L} \frac{0.001}{T_a} \frac{I_c}{4.40 \times 10^{-6}} 0.96 \exp(2\alpha z), \quad (1)$$

where R_L is the Lambertian reflectivity, 0.0041 was the reflectivity of the calibration target, 0.0393 was the pulse energy used in the calibration, E_L is the laser energy for the measurement, 0.001 was the transmission of the absorber used in the calibration, T_a is the transmission of the absorber for the measurement, I_c is the photocathode current measured, 4.40×10^{-6} was the photocathode current measured in the calibration, the factor of 0.96 accounts for the surface loss, α is the attenuation of the lidar signal in the water, and z is the depth. The photocathode currents are obtained from the measured voltage by dividing by the 50 Ω load impedance and by the photomultiplier tube gain. The surface loss occurs because of the 2% reflection each time the light passes through the air-water interface. The lidar attenuation is obtained from the decay of the lidar signal with depth in the vicinity of each school.

The effects of surface roughness on the transmission were considered and found to be negligible. The surface loss was calculated for near-normal incidence but is not very sensitive to incidence angle. Even at an incidence angle of 45° the surface transmission would only change from 0.96 to 0.94. The mean wind speed, taken from the NOAA St Petersburg buoy, was 6.5 m s^{-1} for the first day of flights. From Cox and Munk (1954), we estimate the root-mean-square slope at this wind speed to be about 0.19 or about 11°, so the loss due to large slopes can safely be neglected. From Monahan and Muircheartaigh (1980), we estimate the foam coverage at this wind speed to be about 0.23% and so losses from foam on the surface can also be neglected. Winds on the other days were lighter so these losses would be even smaller.

The volume-backscatter coefficient is easily calculated from the Lambertian reflectivity. In our calculation of the Lambertian reflectivity we are actually measuring backscatter and assuming that the scattering is uniform into π steradians. Thus, recovering backscatter involves dividing the Lambertian reflectivity by π. Converting to volume-backscatter coefficient involves further division by the length of the scattering volume, which is 0.5 cτ/n, where c is the speed of light in vacuum, τ is the pulse length, and n is the index of refraction of seawater. For our pulse length the length of the measurement volume is 1.35 m.

Acoustic data were post-processed using standard, echo-integration (EI) methods (Hewitt and Demer, 1993) as facilitated by SonarData's Echoview (V2.2.50). Echograms showed significant crosstalk from another shipboard echosounder or reverberation from previous transmissions of the survey echosounder or both these possible sources. The resulting intermittent high-intensity noise complicated quantitative EI analyses of these data over large transect distances. However, accurate analyses of individual fish schools could be performed on most schools (e.g. those without noise spikes). The S_v data attributed to fish schools were summed over the vertical extent and averaged over the horizontal extent of the school. This resulted in a nautical area-scattering coefficient (NASC; m^2/nmi^2), or the backscattering cross-sectional area of fish per nautical unit of sea-surface area ($1\ nmi^2 = 3.4299 \times 10^6\ m^2$). The school boundaries were estimated with a S_v threshold = −70 dB. NASC is thought to be proportional to the numerical abundance of fish in the school (Johannesson and Mitson, 1983).

Results

Listed in Table 1 are the letter designators for each school, their GPS coordinates, the number of lidar passes over the schools and the mean Lambertian reflectivities together with their standard deviations when three or more passes were made over a school. In most cases, it was only possible to get one good measurement on each school; co-locating the laser spot with the school was very difficult. The number of acoustic passes over the school, mean S_v, and NASC are also given in Table 1.

While several schools of mullet were targeted by the lidar during the first flight, the boat was positioned over only one school, designated A, with reasonable certainty. Figure 2 is a lidar echogram of this school with the x-axis showing relative flight time in seconds and the y-axis displaying depth in meters. Warmer color values

Table 1. Lidar (column 2–4) and acoustic (column 5–7) data for the fish schools used in this study.

School	Number of passes	Mean reflectivity	Standard deviation	Number of passes	Mean Sv (dB)	NASC (m^2 nmi^{-2})
A	1	2.40×10^{-3}	—	2	−31.02	84 780
B	9	2.14×10^{-3}	7.97×10^{-4}	4	−31.57	208 337
C	6	6.50×10^{-4}	9.63×10^{-5}	14	−37.97	10 992
D	1	5.59×10^{-4}	—	3	−45.14	2 127
E	1	5.35×10^{-4}	—	2	−46.04	2 137
F	1	5.85×10^{-4}	—	4	−43.66	4 639
G	1	4.61×10^{-4}	—	4	−41.49	3 904

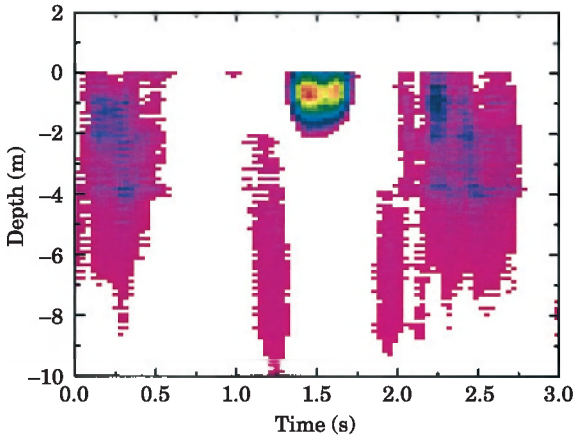

Figure 2. Lidar echogram showing a mullet school near the surface.

represent more lidar signal. The fish school is clearly visible at the surface, starting at 1.5 s. The school was crossed in 11 pulses, which corresponds to a time of 0.37 s. From GPS positions an inferred flight speed of 48 m s^{-1} translates the crossing time to a distance of 18 m. This distance relates to the convolution of the illumination at the surface and the backscatter distribution along the path. With a 5 m spot size at the surface, the school length is estimated to be about 13 m.

Acoustic measurements were made in the same area as the lidar. As a result of rough weather most of the echograms were noisy due to surface turbulence. There was also some acoustic crosstalk with a navigation echosounder aboard the boat. Nevertheless, two passes were made over a large school of mullet measuring approximately 12 m long and 4.5 m high and located at a depth of about 3 to 7.5 m. While the horizontal dimension of the school is similar to that observed with lidar, the vertical position of the school is markedly deeper. This may be caused by fish-avoidance reaction to the survey vessel. It is also possible, although we think it unlikely, that the echosounder and lidar measured different schools. Figure 3 is the acoustic echogram of this school.

On the second flight, one school of mullet, designated B, was found just outside Tampa Bay. Part of the school was netted with a purse seine although most fish escaped through the net opening. Fish sampled by hook-and-line had lengths averaging approximately 41.5 cm.

For both the lidar and echosounder measurements of each school, mean volume backscatter and associated standard deviations are presented in Table 2 and plotted in Figure 4. The linear regression in Figure 4 is:

$$s_v = 1.68\beta(\pi) - 1.55 \times 10^{-4}. \quad (2)$$

The correlation is 0.994. The correlation was also calculated for all combinations of individual lidar and echosounder measurements on each school. The median value of these correlation values was 0.973; 5% were below 0.76 and 5% were above 0.996.

Discussion

The negative y-intercept in Equation (2) indicates that the echosounder reflectivities are systematically lower than the lidar reflectivities. Visual observations from the aircraft suggest that this might be due to fish avoidance of the survey boat. Additional evidence of avoidance in some cases is provided by the depth of the top of the school. Table 3 gives the depths of the tops of the schools as measured by the lidar and by the echosounder. In most cases, the lidar detected fish right up to the surface. Because of the limited depth resolution of the lidar, these fish might be as deep as 20–30 cm. In all cases but one the lidar detected fish closer to the surface than the echosounder. This exception was, at a depth of 2–3 m, the deepest observed by both the lidar and the echosounder. These data are consistent with fish moving down away from the surface when the boat approaches.

The slope of Equation (2) is greater than unity which means that for each fish the acoustic backscatter is larger than the optical backscatter. This is consistent with recent calculations (Churnside *et al.*, 2001b). Lidar target-strength measurements should be made on more species of fish to allow fish-density comparisons to be made.

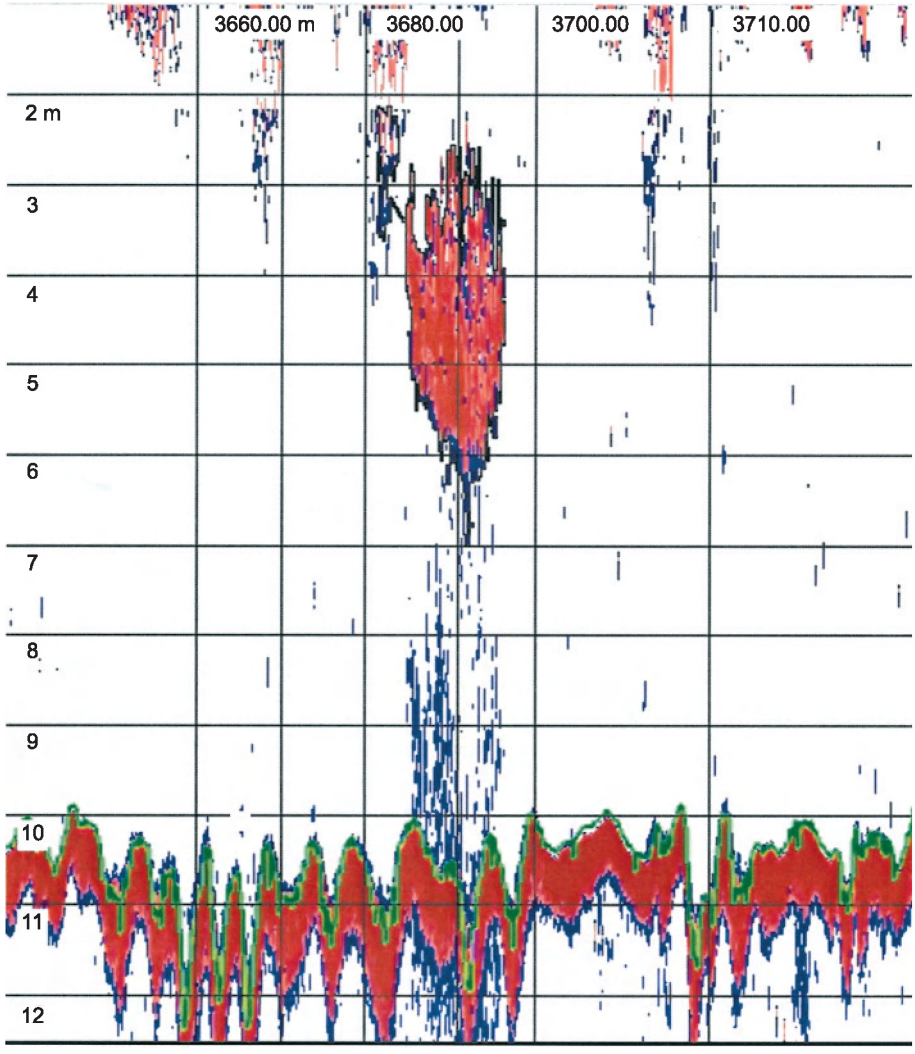

Figure 3. Acoustic echogram of the same mullet school.

Table 2. Lidar and echosounder volume-backscatter coefficients, their respective standard deviations (s.d.), and species identification.

School	Lidar $\beta(\pi)$	s.d.	Acoustic s_v	s.d.	Identification
A	5.66×10^{-4}	—	7.91×10^{-4}	9.63×10^{-5}	Mullet
B	5.04×10^{-4}	1.88×10^{-4}	6.96×10^{-4}	8.77×10^{-5}	Mullet
C	1.53×10^{-4}	2.27×10^{-5}	1.60×10^{-4}	1.50×10^{-4}	Threadfin herring or Spanish sardine
D	1.32×10^{-4}	—	3.07×10^{-5}	9.31×10^{-6}	No identification
E	1.26×10^{-4}	—	2.49×10^{-5}	2.83×10^{-6}	Cigar minnow
F	1.38×10^{-4}	—	4.31×10^{-5}	3.52×10^{-5}	Herring
G	1.09×10^{-4}	—	7.09×10^{-5}	4.08×10^{-5}	Blue runner and Spanish sardine

The last column in Table 2 shows the aerial spotter's estimates for the schools. Although there are some differences for schools with low volume-backscattering coefficients, the strong correlation between s_v and $\beta(\pi)$ holds for a variety of species. The cigar minnows, herring, and one unidentified school have lower s_v to $\beta(\pi)$ ratio than threadfin herring, blue runner, and Spanish sardine.

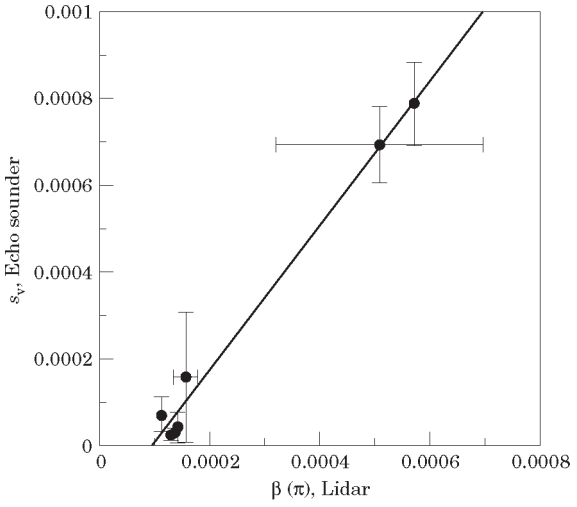

Figure 4. Echosounder volume-backscatter coefficient as a function of lidar volume-backscatter coefficient. Points are mean values, error bars represent standard deviation of the measurements, and the solid line is the least-squares regression, with a correlation coefficient of 0.994.

The data presented here are all from schools of fish very close to the surface. In fact we required that the schools to be visible from the air so that the boat could be directed to the right school. The lidar is not limited to these shallow fish however. Except in a few regions of particularly turbid water near the coast the lidar return from the bottom was observed in water depths up to almost 50 m. An example of this depth penetration is shown in Figure 5, which shows the bottom at about 45 m and a scattering layer, probably plankton from its extent, at a depth of about 30 m.

Table 3. Depth of the top of the schools (in metres) as measured by lidar and by echosounder.

School	Lidar depth	Acoustic depth
A	0	—
B	0	0–1
C	2–3	2–3
D	0.5	2–3
E	1	2–3
F	0	2–3
G	0	9–14

Conclusion

There is a high correlation between the lidar and acoustic reflectivities of fish schools off the west coast of Florida. This implies that airborne lidar may be a very useful tool to survey schools of fish rapidly in this region. With some practice it is possible for a pilot to routinely place the lidar spot on even small fish schools. However, because lidar can also detect schools that are not visible to an aerial spotter and spotters cannot view the vertical extent of a school, statistical surveys such as sets of line transects are more likely candidates for rapid and accurate assessments of fish distributions and abundances.

For schools that are too deep to be visible to the spotter, however, species identification will be a problem

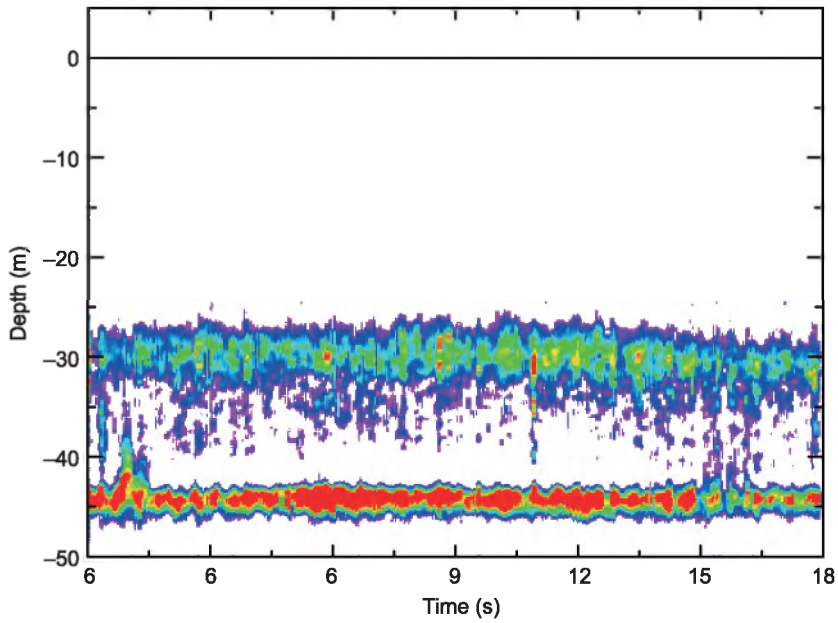

Figure 5. Lidar echogram showing a scattering layer at a depth of 30 m over the bottom at a depth of 45 m.

for lidar-only surveys. Numerous similar species of small schooling fish exist together in this area, and it will be difficult to distinguish between them from the lidar signal alone. In this region, it will probably be necessary to follow aerial surveys with sampling in selected areas to get representative species distributions.

Acknowledgements

This work was partially supported by the Florida Marine Research Institute. We would like to thank the pilots of the NOAA Twin Otter: Lt Carl Newman, Lt Jeff Hagan, Lt Adam Dunbar, Lt Scott Sandorf, and Lt John Longenecker. Steve Leonard, the aerial fish spotter from Osprey Flight Services, Inc., is commended for skilfully locating fish schools and estimating their species content. We thank James J. Wilson, ETL, for collecting the lidar data, Cynthia Meyer, Michael Wessel, and Robert Muller of the Florida Fish and Wildlife Conservation Commission (FFWCC) for collecting the echosounder data, and Jenna Torteorelli and Nicole Dunham, also from FFWCC, for catching and measuring the fish. Thanks also to John Hunter, SWFSC, for facilitating this collaboration.

References

ANSI 1993. Safe Use of Lasers, Standard Z-136.1. American National Standards Institute, New York. 120 pp.

Churnside, J. H., Wilson, J. J., and Tatarskii, V. V. 1997. Lidar profiles of fish schools. Applied Optics, 36: 6011–6020.

Churnside, J. H., Wilson, J. J., and Tatarskii, V. V. 2001a. Airborne lidar for fisheries applications. Optical Engineering, 40: 406–414.

Churnside, J. H., Sawada, K., and Okumura, T. 2001b. A comparison of lidar and echosounder performance in fisheries. Journal of the Marine Acoustic Society of Japan, 28: 49–61.

Cox, C., and Munk, W. 1954. Measurement of the roughness of the sea surface from photographs of the sun's glitter. Journal of the Optical Society of America, 44: 838–850.

Hewitt, R. P., and Demer, D. A. 1993. Dispersion and abundance of Antarctic krill in the vicinity of Elephant Island in the 1992 austral summer. Marine Ecological Progress Series, 99: 29–39.

Johannesson, K. A., and Mitson, R. B. 1983. Fisheries Acoustics: A practical manual for aquatic biomass estimation. Food and Agriculture Organization Technical Paper 240. Food and Agriculture Organization of the United Nations, Rome. 249 pp.

Krekova, M. K., Krekov, G. M., Samokhvalov, I. V., and Shamanaev, V. S. 1994. Numerical evaluation of the possibilities of remote sensing of fish schools. Applied Optics, 33: 5715–5720.

Monahan, E. C., and Muircheartaigh, I. O. 1980. Optimal power-law description of oceanic whitecap coverage dependence on wind speed. Journal of Physical Oceanography, 10: 2094–2099.

Shifrin, K. S. 1988. Physical Optics of Ocean Water. American Institute of Physics, New York. 21 pp.

Squire, J. L. Jr, and Krumboltz, H. 1981. Profiling pelagic fish schools using airborne optical lasers and other remote sensing techniques. Marine Technological Society Journal, 15: 27–31.

Zorn, H. M., Churnside, J. H., and Oliver, C. W. 2000. Laser safety thresholds for cetateans and pinnipeds. Marine Mammal Science, 16: 186–200.